Journal of Physics: Conference Series

A multi-resolution computational method to solve highly non-linear inverse scattering problems

A multi-resolution computational method to solve highly non-linear inverse scattering problems

Marco Salucci [1], Alessandro Polo [1], Kuiwen Xu [2], and Yu Zhong [3]

[1] ELEDIA Research Center (ELEDIA@UniTN - University of Trento), I-38123 Trento, Italy
[2] Key Lab of RF Circuits and Systems of Ministry of Education, Hangzhou Dianzi University, Hangzhou, China
[3] Institute of High Performance Computing, A*STAR, Singapore

E-mail: marco.salucci@unitn.it

Abstract. An innovative computational method to solve inverse scattering problems is proposed for retrieving the electromagnetic properties of unknown targets. The proposed technique is based on the contraction integral equation for inversion (*CIE-I*) method to mitigate multiple scattering contributions when imaging strong scatterers. More specifically, the *CIE-I* is integrated in an effective multi-resolution (*MR*) scheme to reduce the ratio between unknowns and non-redundant data as well as to exploit iteratively acquired information on the scenario for yielding higher-resolution reconstructions. Some preliminary numerical results are reported to assess the capabilities of the proposed *MR-CIE-I* method.

1. Introduction

When microwave imaging strong scatterers, the high *non-linearity* of the inverse scattering problem at hand has to be carefully dealt with to faithfully recover the dielectric profile of the domain under test [1]. In the state-of-the-art literature, many efforts have been made to properly cope with the non-linearity arising in many applicative scenarios including non-destructive testing and evaluation [2], through-wall imaging [3], ground penetrating radar subsurface investigations [4]-[6], and medical imaging [7]-[12].

Linear approximations of the inverse scattering equations (e.g., Born or Rytov [13][14]) are an effective recipe to restore linearity, but the price to pay is the limitation to deal with only weak scatterers and the impossibility to provide accurate material characterizations. On the other hand, fully non-linear approaches have been proposed by exploiting stochastic optimization tools such as genetic algorithms (*GA*s), particle swarm optimization (*PSO*), and differential evolution (*DE*) due to their intrinsic capability of escaping from multiple local minima present in the data-mismatch cost function to be minimized. However, these methodologies cause a very high computational burden when applied to high-dimensional solution spaces [6]. Otherwise, it is worth remarking that the non-linearity of the inverse scattering problem can be partially mitigated by reducing the cardinality of the inversion problem. For instance, multi-resolution (*MR*) inversion schemes have been successfully adopted to keep as low as possible the ratio between sought unknowns and informative/non-redundant data. Within this framework, a profitable integration of stochastic as well as deterministic methods within a *MR* strategy can enable accurate and computationally-efficient inversions [4][6][15]. Recently, a new formulation has been introduced to mathematically model highly non-linear inverse scattering problems. This approach is based on the contraction integral equation for inversion (*CIE-I*) [16]. The *CIE-I* allows to effectively reduce the non-linearity with respect to a standard Lippmann-Schwinger integral equation (*LSIE*) formulation, thus the imaging of high contrast and/or large (in terms of wavelengths) targets [16] is expected to be more effective. Accordingly, this work is aimed at presenting an innovative inversion methodology based on the integration of the *CIE-I* method within a *MR* inversion scheme to effectively/efficiently deal with strong scatterers. More in detail, Section 2 describes the mathematical formulation of the addressed problem as well as the proposed *MR-CIE-I* methodology to solve it. Some numerical results and comparisons against competitive alternatives are given in Section 3, while some final remarks and observations are drawn in Section 4.

2. Mathematical Formulation

Let us consider a $2D$ inverse scattering scenario in which a set of V plane waves with transverse-magnetic polarization is exploited to probe an investigation domain Ω. It is assumed that the electromagnetic characteristics of the background medium are known and equal to those of free-space (ε_0 and μ_0). Moreover, Ω includes an unknown non-magnetic target with isotropic relative permittivity ε_T and conductivity σ_T. Under these assumptions, the arising scattering phenomena at angular frequency ω [1] can be modeled through the following *LSIE*

$$\mathcal{I}_v(x, y) = \mathcal{E}_v(x, y) - \int_\Omega \mathcal{G}(x, y; x', y')\, \tau(x', y')\, \mathcal{E}_v(x', y')\, dx'dy' \qquad (x, y) \in \Omega;\ v = 1, ..., V \tag{1}$$

where $\mathcal{E}_v(x, y)$ and $\mathcal{I}_v(x, y)$ are the v-th total and incident electric fields, respectively, while $\mathcal{G}(x, y; x', y')$ is the free-space Green's function for the *2D* scattering problem at hand. Moreover, $\tau(x, y)$ is the contrast function, mathematically modeling the presence of the target as a discontinuity of the electromagnetic properties inside Ω

$$\tau(x, y) = \varepsilon_r(x, y) - 1; \quad (x, y) \in \Omega \tag{2}$$

$\varepsilon_r(x, y)$ being the complex relative permittivity at position $(x, y) \in \Omega$. According to the contrast source inversion (*CSI*) formulation [17], it is then possible to express the v-th contrast source as follows

$$\mathcal{J}_v(x, y) = \tau(x, y)\, \mathcal{E}_v(x, y); \quad (x, y) \in \Omega;\ v = 1, ..., V \tag{3}$$

and re-write accordingly the *state* equation (1) as

$$\tau(x, y)\, \mathcal{I}_v(x, y) = \mathcal{J}_v(x, y) - \tau(x, y) \int_\Omega \mathcal{G}(x, y; x', y')\, \mathcal{J}_v(x', y')\, dx'dy' \qquad (x, y) \in \Omega;\ v = 1, ..., V. \tag{4}$$

Furthermore, the scattered field, expressed as the difference between the total and incident fields, complies with the following data *LSIE* equation

$$\mathcal{S}_v(x, y) = [\mathcal{E}_v(x, y) - \mathcal{I}_v(x, y)] = \int_\Omega \mathcal{G}(x, y; x', y')\, \mathcal{J}_v(x', y')\, dx'dy' \qquad (x, y) \in \Lambda;\ v = 1, ..., V \tag{5}$$

Λ being a suitably-defined external observation domain.

In order to mitigate the non-linearity of the inverse scattering problem at hand, the *CIE-I* formulation is exploited [16]. Accordingly, (4) is multiplied by the following function

$$\chi(x, y)\, [\chi(x, y)\, \tau(x, y) + 1]^{-1} \tag{6}$$

[1] A time factor $\exp(j\omega t)$ is assumed.

where $\chi(x, y)$ is the local *CIE-I* regularization term, resulting in

$$\begin{aligned}\chi(x, y)\,\mathcal{J}_v(x, y) = \mathcal{W}(x, y)\,\chi(x, y)\,\mathcal{J}_v(x, y) + \mathcal{W}(x, y)\\ \times\left[\mathcal{I}_v(x, y) + \int_\Omega \mathcal{G}(x, y; x', y')\,\mathcal{J}_v(x', y')\,dx'dy'\right]\\ (x, y) \in \Omega;\ v = 1, \ldots, V\end{aligned} \tag{7}$$

where

$$\mathcal{W}(x, y) = \tau(x, y)\,\chi(x, y)\left[\chi(x, y)\,\tau(x, y) + 1\right]^{-1} \tag{8}$$

is the *modified CIE-I* contrast function [16].
In order to solve the *CIE-I* problem described by (5) and (7), as well as to further counteract non-linearity and ill-posedness, a multi-resolution (MR) scheme is adopted to (a) keep as low as possible the ratio between unknowns and data, as well as to (b) exploit progressively acquired information on the solution.

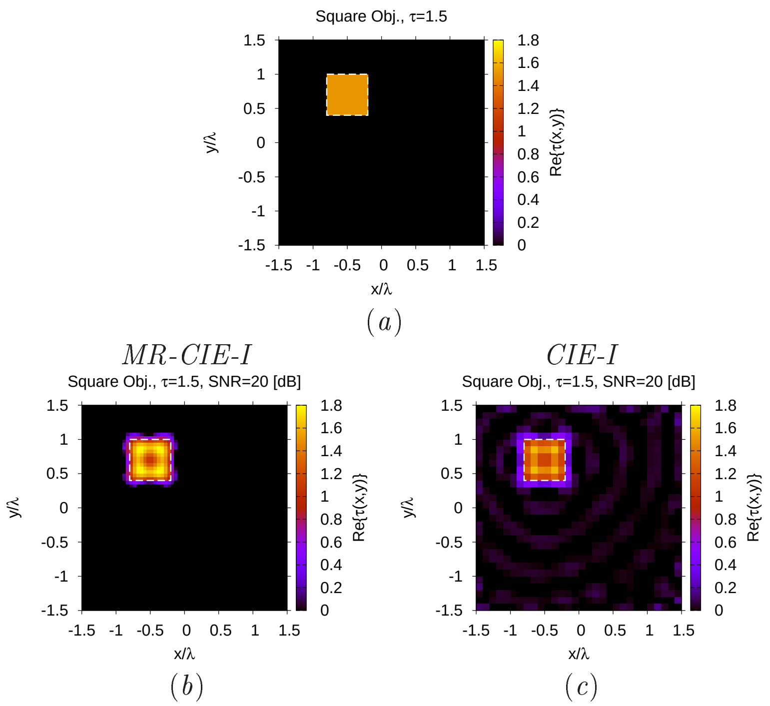

Figure 1. *Numerical Results* (*Square Profile*, $\tau = 1.5$, $SNR = 20$ [dB]) - (a) Actual and retrieved contrast function by the (b) *MR-CIE-I* and (c) *CIE-I* methods.

More in detail, the following iterative procedure of S steps is adopted

(i) *Initialization* ($s = 0$) - Discretize Ω into N square cells, N being properly selected according to the degrees-of-freedom theory for the scenario at hand [4];

(ii) *Low Order Inversion* ($s = 1$) - Solve the *CIE-I* problem (5), (7) exploiting the subspace optimization method (SOM) as a computationally-fast core solver with regularization capabilities [18]. Then, let $s \leftarrow (s + 1)$ and proceed to Step (iii)(a);

(iii) *MR Loop* ($s = 2, \ldots, S$)

  (a) Apply the "filtering and clustering" procedure [4] to update the region of interest $\Omega_s \subset \Omega_{s-1}$ ($\Omega_1 = \Omega$). Then, discretize it into N square sub-domains and map the solution found at the $(s-1)$-th step to form the initial guess for the successive inversion stage;

(b) Solve the *CIE-I* problem (5), (7) through the *SOM* to retrieve a higher-resolution guess of the s-th region of interest;

(c) Terminate the zooming procedure when the maximum number of steps has been reached ($s = S$), or if a stationary condition on Ω_s size and location is met. Otherwise, let $s \leftarrow (s+1)$ and go to Step (iii)(a);

(iv) *Output Phase* - Output the retrieved solution at the last performed *MR* step.

3. Preliminary Numerical Validation

In this Section, some numerical results are shown to preliminarily assess the effectiveness of the proposed *MR-CIE-I* inversion scheme. Towards this end, a square investigation domain Ω of side 3λ, λ being the free-space wavelength, has been successively probed by $V = 27$ plane waves impinging from angular directions $\phi_v = [2\pi (v-1)/V]$, $v = 1, ..., V$, the scattered fields being collected by $M = 27$ ideal field probes uniformly distributed over a circular observation domain Λ of radius 2.12λ. As for the settings of the *MR-CIE-I*, the number of sub-domains has been set to $N = 324$, while an additive white Gaussian noise has been added to the scattered data in order to test the robustness of the proposed method.

Figure 1 shows the *MR-CIE-I* inversion results when dealing with the retrieval of the square profile of Fig. 1(a), having a contrast function of $\tau = 1.5$ (processing noisy data at $SNR = 20$ [dB]). As it can be observed, the *MR-CIE-I* provides a faithful reconstruction of the target shape and electromagnetic properties [Fig. 1(b) vs. Fig. 1(a)]. Moreover, there is a visible improvement in terms of reconstruction accuracy with respect to a standard single-resolution (*SR*) *SOM*-based implementation (i.e., the *CIE-I* [16]), this latter yielding an under-estimation of the actual contrast and many artifacts in the background region [Fig. 1(c) vs. Fig. 1(b)].

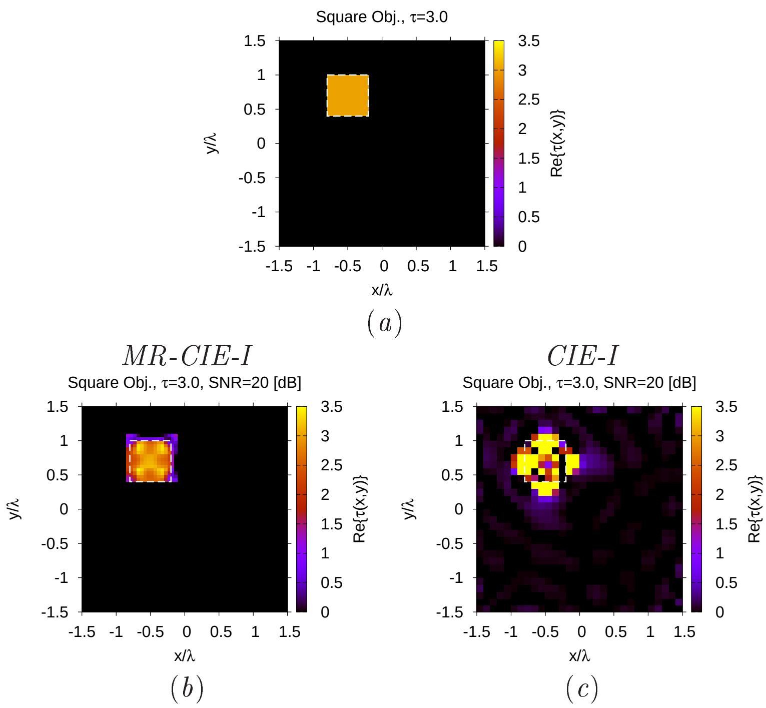

Figure 2. *Numerical Results* (*Square Profile*, $\tau = 3.0$, $SNR = 20$ [dB]) - (a) Actual and retrieved contrast function by the (b) *MR-CIE-I* and (c) *CIE-I* methods.

Such positive outcomes are further confirmed when increasing the actual permittivity of the

scatterer. As a matter of fact, when $\tau = 3.0$ [$\varepsilon_T = 4.0$ - Fig. 2(a)], a remarkable improvement of the inversion quality has been obtained by the *MR-CIE-I* over the *CIE-I* thanks to its effectiveness in mitigating the strong non-linearity of the problem, regardless of the presence of a non-negligible noise on processed data [Fig. 2(b) vs. Fig. 2(c)].
Previous outcomes are confirmed by the values of the total integral error [6] as a function of the actual contrast value (Fig. 3). Indeed, it can be observed that the error increases (as expected) with τ since higher contrasts lead to higher non-linearities.

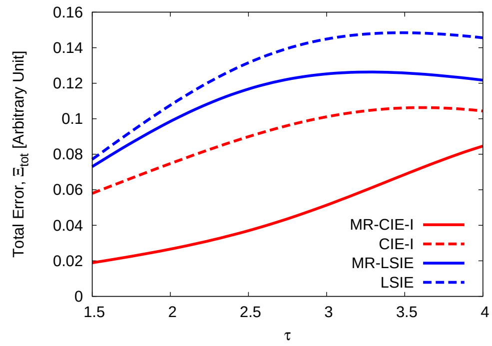

Figure 3. *Numerical Results* (*Square Profile*, $SNR = 20$ [dB]) - Behavior of the total integral error as a function of the actual contrast value for the *MR-CIE-I*, *CIE-I*, *MR-LSIE*, and *LSIE* methods.

Finally, it is worth observing that the *MR-CIE-I* overcomes a state-of-the-art *MR*-based solution exploiting a standard *CSI-LSIE* formulation of the inverse scattering problem (i.e., the *MR-LSIE* [15]). Figure 4(a) reports the result yielded by the *MR-LSIE* to point out its inability to recover a correct guess of the target despite the use of a *MR* procedure (only some "rings" appear around the object support). For completeness, the single-resolution *LSIE* solution [18] has been reported [Fig. 4(b)], as well, while the integral errors of both *LSIE* methods have been added in Fig. 3 to have a wider overview of the reconstruction capabilities of the proposed method over state-of-the-art alternatives.

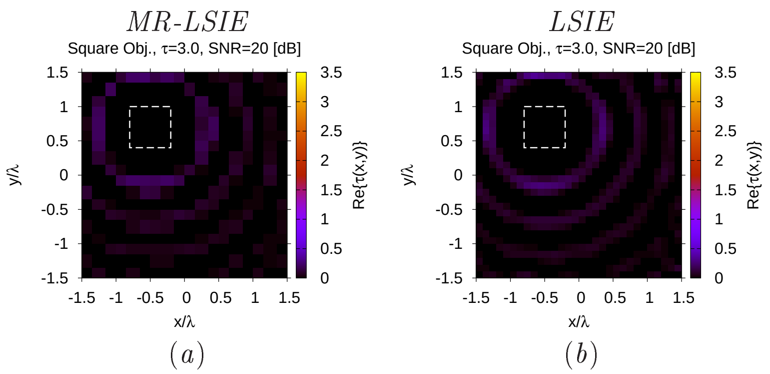

Figure 4. *Numerical Results* (*Square Profile*, $\tau = 3.0$, $SNR = 20$ [dB]) - Retrieved contrast function by the (a) *MR-LSIE* and (b) *LSIE* methods.

4. Conclusions

An innovative computational method to solve highly non-linear inverse scattering problems has been presented. The proposed method effectively combines the regularization and linearization capabilities of the *CIE-I* formulation with those of a *MR* scheme, improving the resolvability against the non-linearity of the concerned problems. Reported preliminary numerical results indicate that the *MR-CIE-I* yields faithful reconstructions of the electromagnetic properties of the imaged domain, with good robustness to noise. Moreover, it has been shown that the proposed method outperforms the *CIE-I* method as well as two state-of-the-art solutions based on the *LSIE* (even when regularizations are employed), especially when dealing with the retrieval of strong scatterers. Future works will be aimed at extending the proposed method to deal with fully three-dimensional scenarios, with applications to both subsurface and biomedical imaging.

Acknowledgments
This work benefited from the networking activities carried out within the SNATCH Project (2017-2019) funded by the Italian Ministry of Foreign Affairs and International Cooperation, Directorate General for Cultural and Economic Promotion and Innovation, and the Project "CYBER-PHYSICAL ELECTROMAGNETIC VISION: Context-Aware Electromagnetic Sensing and Smart Reaction (EMvisioning)" funded by the Italian Ministry of Education, University, and Research within the PRIN2017 Program.

References
[1] Chen X 2018 *Computational Methods for Electromagnetic Inverse Scattering* (Singapore: Wiley-IEEE)
[2] Zoughi R 2000 *Microwave Nondestructive Testing and Evaluation* (Amsterdam, The Netherlands: Kluwer)
[3] Xu K, Zhong Y, Chen X and Lesselier D 2018 A fast integral equation-based method for solving electromagnetic inverse scattering problems with inhomogeneous background *IEEE Trans. Antennas Propag.* **66** 4228-4239
[4] Salucci M, Poli L and Massa A 2017 Advanced multi-frequency GPR data processing for non-linear deterministic imaging *Signal Proc.* **132** 306-318
[5] Cui T, Chew WC, Aydiner AA and Chen S 2001 Inverse scattering of two-dimensional dielectric objects buried in a lossy earth using the distorted Born iterative method *IEEE Trans. Geosci. Remote Sens.* vol. **39** 339-346
[6] Salucci M, Poli L, Anselmi N and Massa A 2017 Multifrequency particle swarm optimization for enhanced multiresolution GPR microwave imaging *IEEE Trans. Geosci. Remote Sens.* **55** 1305-1317
[7] Salucci M, Gelmini A, Vrba J, Merunka I, Oliveri G and Rocca P 2019 Instantaneous brain stroke classification and localization from real scattering data *Microw. Opt. Technol. Lett.* **61** 805-808
[8] Song X, Li M, Yang F, Xu S and Abubakar A 2019 Study on joint inversion algorithm of acoustic and electromagnetic data in biomedical imaging *IEEE J. Multiscale and Multiphys. Comput. Techn.* **4** 2-11
[9] Abubakar A, van den Berg PM and Mallorqui J 2002 Imaging of biomedical data using a multiplicative regularized contrast source inversion method *IEEE Trans. Microw. Theory Techn.* **50** 1761- 1771
[10] Song X, Li M, Yang F, Xu S and Abubakar A 2019 Study on joint inversion algorithm of acoustic and electromagnetic data in biomedical imaging *IEEE J. Multiscale Multiphys. Comput. Techn.* **4** 2-11
[11] Mojabi P and LoVetri J 2009 Microwave biomedical imaging using the multiplicative regularized Gauss-Newton inversion *IEEE Antennas Wireless Propag. Lett.* **8** 645-648
[12] Salucci M, Oliveri G and Massa A 2019 Real-time electrical impedance tomography of the human chest by means of a learning-by-examples method *IEEE Journal of Electromagnetics, RF, and Microwaves in Medecine and Biology* (*in press*) (DOI: 10.1109/JERM.2019.2893217)
[13] Slaney M, Kak AC and Larsen LE 1984 Limitations of imaging with first-order diffraction tomography *IEEE Trans. Microw. Theory Techn.* **32** 860-874
[14] Shumakov D and Nikolova N 2018 Fast quantitative microwave imaging with scattered-power maps *IEEE Trans. Microw. Theory Techn.* **66** 439-449
[15] Oliveri G, Zhong Y, Chen X and Massa A 2011 Multiresolution subspace-based optimization method for inverse scattering problems *J. Opt. Soc. Am. A* **28** 2057-2069
[16] Zhong Y, Lambert M, Lesselier D and Chen X 2016 A new integral equation method to solve highly nonlinear inverse scattering problems *IEEE Trans. Antennas Propag.* **64** 1788-1799
[17] Li M, Abubakar A and Van Den Berg P M 2009 Application of the multiplicative regularized contrast source inversion method on 3D experimental Fresnel data *Inverse Probl.* **25** 1-23
[18] Chen X 2010 Subspace-based optimization method for solving inverse-scattering problems *IEEE Trans. Geosci. Remote Sens.* **48** 42-49